

A novel approach in the WIMP quest: Cross-Correlation of Gamma-Ray Anisotropies and Cosmic Shear

Stefano Camera,¹ Mattia Fornasa,² Nicolao Fornengo,³ and Marco Regis³

¹*CENTRA, Instituto Superior Técnico, Universidade Técnica de Lisboa, Lisboa, Portugal*

²*School of Physics and Astronomy, University of Nottingham, Nottingham, United Kingdom*

³*Dipartimento di Fisica, Università di Torino and INFN, Torino, Italy*

(Dated: December 21, 2012)

Both cosmic shear and cosmological gamma-ray emission stem from the presence of Dark Matter (DM) in the Universe: DM structures are responsible for the bending of light in the weak lensing regime and those same objects can emit gamma-rays, either because they host astrophysical sources (active galactic nuclei or star-forming galaxies) or directly by DM annihilations (or decays, depending on the properties of the DM particle). Such gamma-rays should therefore exhibit strong correlation with the cosmic shear signal. In this Letter, we compute the cross-correlation angular power spectrum of cosmic shear and gamma-rays produced by the annihilation/decay of Weakly Interacting Massive Particle (WIMP) DM, as well as from astrophysical sources. We show that this observable provides novel information on the composition of the Extra-galactic Gamma-ray Background (EGB), since the amplitude and shape of the cross-correlation signal strongly depends on which class of source is responsible for the gamma-ray emission. If the DM contribution to the EGB is significant (at least in a definite energy range), although compatible with current observational bounds, its strong correlation with the cosmic shear makes such signal potentially detectable by combining Fermi-LAT data with forthcoming galaxy surveys, like Dark Energy Survey and Euclid. At the same time, the same signal would demonstrate that the weak lensing observables are indeed due to particle DM matter and not to possible modifications of General Relativity.

PACS numbers: 95.35.+d, 95.30.Sf, 98.62.Sb, 98.80.-k, 95.85.Pw

Introduction. Weak gravitational lensing refers to the small distortions of images of distant galaxies, produced by the distribution of matter located between galaxies and the observer [1–4]. Contrary to strong lensing, where distortion is caused by a small number of massive objects, weak lensing studies aim at reproducing the statistical properties of the density field acting as a lens, as well as investigating the geometrical properties of the Universe. A distorted image can be described by the so-called distortion matrix, normally parametrized in terms of the convergence κ (controlling modifications in the size of the image) and the shear γ (accounting for shape distortions). Whilst the former is a direct estimator of matter density fluctuations along the line of sight, the latter is easier to measure, through correlations in the observed source ellipticities. In the flat-sky approximation, the two generate identical angular power spectra: we shall thus focus on the shear as an estimator of the convergence, and, from now on, we indicate with κ the observables related to cosmic shear.

The auto-correlation between the gravitational shear in two different directions can provide information on the clustering of the large scale structures responsible for the lensing effect. The technique has already been used in [5–8] where data of the COSMOS galaxy survey allow for a measurement of the two-point correlation function (2PCF) of the shear at angular scales between 0.1 and 10 arcmin. Future surveys, like Pan-STARRS, Dark Energy Survey (DES) [9] and Euclid [10], due to their larger coverage and improved sensitiv-

ities, will be able to reconstruct two-dimensional shear maps, from which one can extract the auto-correlation angular power spectrum (PS).

The same Dark Matter (DM) structures that act as lenses can themselves emit light at various wavelengths, including the γ -ray range. While γ -rays can be produced by astrophysical sources hosted by DM halos (i.e., star-forming galaxies (SFG), or active galactic nuclei (AGN)), DM itself may be a source of γ -rays, through its self annihilation or decay, depending on the properties of the DM particle. Those γ -rays emitted by DM should therefore have the potential to exhibit strong correlation with the gravitational lensing signal.

In this Letter we propose to study the cross-correlation of gravitational shear with the Extra-galactic Gamma-ray Background (EGB), i.e., the residual radiation contributed by the cumulative emission of *unresolved* γ -ray sources, as a novel and potentially relevant channel of DM investigation.

The most recent measurement of the EGB was performed by the Fermi-LAT telescope in [11], covering a range between 200 MeV and 100 GeV: the emission is obtained by subtracting the contribution of resolved sources (both point-like and extended) and the Galactic foreground (due to cosmic rays interaction with the interstellar medium) from the whole Fermi-LAT data. Unresolved astrophysical sources like blazars [12–14], SFGs [15, 16] or radio galaxies [17, 18] contribute to the EGB but the exact amount of their contribution is still unknown. γ -rays produced by DM annihilation or

decay can also contribute to EGB [19–23]. However, the fact that the EGB energy spectrum is compatible with a power-law, without any evident spectral feature, suggests that DM cannot play a leading role in the whole energy range [24, 25]. In the angular anisotropies of the EGB emission, the DM also plays a subdominant role: indeed, a detection of a significant auto-correlation angular PS has been recently reported [26] (for multipoles $\ell > 100$, which is the range of interest for our analysis since the contamination of the Galactic foreground can be neglected), but the features of such a signal (in particular its independence on multipole and energy) seem to indicate an interpretation in terms of blazars [27, 28].

Both cosmic shear and γ -ray emission depend on the large scale structure of the Universe, either because this is what generates the lensing effect or because those same structures can produce γ -rays, hosting astrophysical sources, or directly from DM annihilation/decay. A certain level of cross-correlation between cosmic shear and γ -ray emission is therefore expected. The key point of our analysis is to understand whether the shear/ γ -rays cross-correlation is within reach of future galaxy surveys, as DES and Euclid, and under which circumstances such signal can be proficiently used to disentangle a true DM signal from the other astrophysical γ -rays sources. It is the first time, to our knowledge, that such analysis is performed. If successful, this approach could provide direct evidence that what is measured by weak lensing surveys is indeed due to DM and is not, for instance, a manifestation of alternative theories of gravity. We will show in the following that in the case of a significant DM contribution to the EGB (at least in a definite energy range), although compatible with current observational bounds, the strong correlation of the γ -rays emission with cosmic shear makes the DM signal potentially detectable by combining Fermi-LAT measurements with DES and Euclid. A strategy could then be envisaged to use the cross-correlation results to extract information on the DM particle properties (namely its mass and annihilation cross section or decay lifetime [44]).

On more general grounds, this approach can also provide valuable information on the clustering of the matter field and on the properties of galaxies, complementary to what can be deduced from the study of the shear or γ -ray auto-correlations alone. Both the normalization and the shape of the cross-correlation angular PS will depend on which class of sources is considered as responsible for the γ -ray emission and, as a consequence, any detection of cross-power can potentially provide information on the composition of the EGB.

Theoretical modeling. The source intensity along a given direction \vec{n} can be written as:

$$I_g(\vec{n}) = \int d\chi g(\chi, \vec{n}) \tilde{W}(\chi), \quad (1)$$

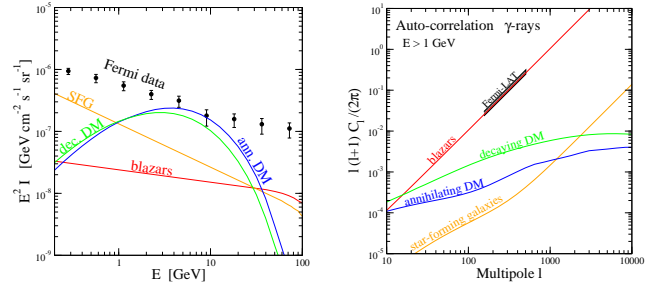


FIG. 1. *Left:* EGB emission as a function of observed energy for the four extragalactic components described in the text. Data are from [11]. *Right:* γ -ray angular PS at $E > 1$ GeV for the same models of the left panel. The observed angular PS is summarized by the black band [26].

where $\chi(z)$ is the radial comoving distance, g is the density field of the source, and \tilde{W} is the window function (which does not depend on \vec{n}). We then define a normalized version $W = \langle g \rangle \tilde{W}$, so $\langle I_g \rangle = \int d\chi W(\chi)$. Expanding the intensity fluctuations of two source populations i and j in spherical harmonics, one can compute (see Appendix) the cross-correlation angular PS (here in the dimensionless form):

$$C_\ell^{(ij)} = \frac{1}{\langle I_i \rangle \langle I_j \rangle} \int \frac{d\chi}{\chi^2} W_i(\chi) W_j(\chi) P_{ij}(k = \ell/\chi, \chi). \quad (2)$$

The definition of the 3-dimensional PS P_{ij} is $\langle \hat{f}_{g_i}(\chi, \mathbf{k}) \hat{f}_{g_j}^*(\chi', \mathbf{k}') \rangle = (2\pi)^3 \delta^3(\mathbf{k} - \mathbf{k}') P_{ij}(k, \chi, \chi')$, where $f_g \equiv [g(\mathbf{x}|m, z)/\bar{g}(z) - 1]$ (\hat{f}_g is its Fourier transform) and the Limber approximation ($k = \ell/\chi$) is assumed to hold. We consider the sources to be characterized by a parameter m (typically the mass), and $g(\mathbf{x}|m)$ is the density field of an object associated to m , while $\bar{g}(z) = \langle g(\vec{n}, z) \rangle$. P_{ij} can be computed following the so-called halo-model approach. The two-point correlation is given by the sum of two components, the 1-halo and 2-halo terms, i.e. $P_{ij} = P_{ij}^{1h} + P_{ij}^{2h}$ [29–31]:

$$P_{ij}^{1h}(k) = \int dm \frac{dn}{dm} \hat{f}_i^*(k|m) \hat{f}_j(k|m) \quad (3)$$

$$P_{ij}^{2h}(k) = \left[\int dm_1 \frac{dn}{dm_1} b_i(m_1) \hat{f}_i^*(k|m_1) \right] \times \left[\int dm_2 \frac{dn}{dm_2} b_j(m_2) \hat{f}_j(k|m_2) \right] P^{\text{lin}}(k), \quad (4)$$

where dn/dm is the number density distribution of sources, P^{lin} is the linear matter PS, and $b_i(m)$ is the linear bias between the object i and matter. Note that the average of $\langle g \rangle$ is given by:

$$\bar{g}(z) = \langle g(\vec{n}, z) \rangle = \int dm \frac{dn}{dm} \int d^3\mathbf{x} g(\mathbf{x}|m, z), \quad (5)$$

which implies that at small k (where $\hat{f} \sim \int d^3\mathbf{x} g(\mathbf{x}|m)/\bar{g}$) the terms in the square-brackets in

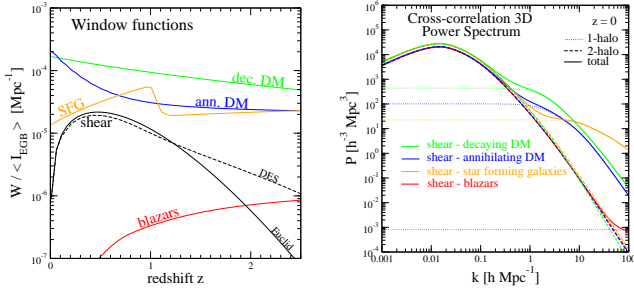


FIG. 2. *Left:* Window functions vs. redshift. For γ -ray sources we consider the flux above 1 GeV normalized to the total EGB intensity measured by Fermi-LAT. *Right:* Three-dimensional PS of cross-correlation shear/ γ -rays at $z = 0$.

Eq. (4) are ~ 1 (except in the case of a significant bias). The 2-halo term is thus normalized to the standard linear matter PS at small k , which motivates the normalization of the window function introduced above.

We aim at cross-correlating the shear signal (source i in Eqs. (2–4)) with γ -rays emitted by DM, SFGs, and blazars (source j in Eqs. (2–4)). For what concerns weak lensing, W takes the form (see, e.g., [4]):

$$W^\kappa(\chi) = \frac{3}{2} H_0^2 \Omega_m [1 + z(\chi)] \chi \int_\chi^\infty d\chi' \frac{\chi' - \chi}{\chi'} \frac{dN}{d\chi'}(\chi')$$

and $dN/d\chi$ represents the redshift distribution of the sources, normalized to unity area (such that we can take $\langle I_i \rangle = 1$ in Eq. (2)). For Euclid $dN/dz = A_E z^2 e^{-(z/z_0)^{1.5}}$, where $z_0 = z_m/1.4$ with $z_m = 0.9$ being the median redshift of the survey and A_E is fixed by the normalization $\int dz dN/dz = 1$. For DES, $dN/dz = A_D (z^a + z^{ab})/(z^b + c)$, with a , b , and c provided in Table 1 of [32], and A_D fixed by the normalization. Since gravitational lensing is sourced by the potential wells of the large scale structure, whose Poisson equation relates to the matter distribution ρ , we have $g_\kappa(\mathbf{x}) = \rho(\mathbf{x})$, and $f_\kappa(\mathbf{x})$ is given by the density contrast $\delta(\mathbf{x})$. For the bias in Eq. (4) we use the estimates in [33]. We adopt the halo mass function dn/dm of [34], the halo concentration from [35], and a NFW halo density profile [36].

For the case of γ -rays from decaying DM we again have $f_d(\mathbf{x}) = \delta(\mathbf{x})$ (we assume $\rho_m \simeq \rho_{DM}$). The window function is now given by:

$$W^{\gamma d}(E_\gamma, z) = \frac{1}{4\pi} \frac{\Omega_{DM} \rho_c}{m_\chi \tau_d} J_d(E_\gamma, z), \quad (6)$$

where m_χ and τ_d are the mass and decay lifetime of the DM particle, $J_d = \int_{E_\gamma}^\infty dE \frac{dN_d(E(1+z))}{dE} e^{-\tau(E(1+z), z)}$ with $dN_d/dE(E)$ being the number of γ -ray photons emitted per decay in $(E, E + dE)$, and τ being the optical depth for absorption [37]. Note that the factor $\Omega_{DM} \rho_c$ comes from the normalization of W , since in this case $\langle g_d \rangle = \bar{\rho}$.

The DM annihilation signal scales with ρ^2 , thus we have $\hat{f}_a \equiv \tilde{u}(k|m)$ given by the Fourier transform of $\rho^2(\mathbf{x}|m)/\langle \rho^2 \rangle$. In the literature, equations are often written in terms of the so-called clumping factor:

$$\Delta^2(z) = \frac{\langle \rho^2 \rangle}{\bar{\rho}^2} = \int_{m_{\min}}^{m_{\max}} dm \frac{dn}{dm} \int d^3\mathbf{x} \frac{\rho^2(\mathbf{x}|m)}{\bar{\rho}^2}, \quad (7)$$

and the window function has the form:

$$W^{\gamma a}(E_\gamma, z) = \frac{(\Omega_{DM} \rho_c)^2}{4\pi} \frac{(\sigma_a v)}{2m_\chi^2} (1+z)^3 \Delta^2(z) J_a(E_\gamma, z),$$

where $(\sigma_a v)$ is the velocity-averaged annihilation rate (which we assume to be the same in all halos) and $J_a = \int_{E_\gamma}^\infty dE \frac{dN_a(E(1+z))}{dE} e^{-\tau(E(1+z), z)}$ with $dN_a/dE(E)$ being the number of γ -ray photons emitted per annihilation in the energy range $(E, E + dE)$. In the annihilating DM case, the predictions for both the window function and the PS heavily depend on the (unknown) clustering at small masses (i.e., on the minimum halo mass, concentration below approximately $10^6 M_\odot$, and on the amount of substructures). We consider $m_{\min} = 10^{-6} M_\odot$ (typical free-streaming mass for WIMPs) and include unresolved subhalos following the scheme described in [38] with parameters tuned as in the HIGH scenario of Sec. 3.3 in [23] (within our halo model, it induces only moderate boost factor ~ 2).

The formalism sketched in Eqs. (1–5) can be used also for a population of astrophysical sources, by replacing the mass with the source luminosity \mathcal{L} as the characterizing parameter. This leads to the replacement of $dm dn/dm$ with $d\mathcal{L} \Phi$, where Φ is the γ -ray luminosity function (GLF). For the range of multipoles of interest ($\ell < 10^3$) both blazars and SFG can be approximated as point sources and we have $g_S(\mathcal{L}, \mathbf{x} - \mathbf{x}') = \mathcal{L} \delta^3(\mathbf{x} - \mathbf{x}')$, which leads to:

$$P_{\kappa\gamma S}^{1h}(k, z) = \int_{\mathcal{L}_{\min}(z)}^{\mathcal{L}_{\max}(z)} d\mathcal{L} \Phi(\mathcal{L}, z) \frac{\mathcal{L}}{\langle g_S \rangle} \tilde{v}(k|m(\mathcal{L}))$$

$$P_{\kappa\gamma S}^{2h}(k, z) = \left[\int_{\mathcal{L}_{\min}(z)}^{\mathcal{L}_{\max}(z)} d\mathcal{L} \Phi(\mathcal{L}, z) b_S(\mathcal{L}, z) \frac{\mathcal{L}}{\langle g_S \rangle} \right] \times \left[\int_{m_{\min}}^{m_{\max}} dm \frac{dn}{dm} \tilde{v}(k|m) \right] P^{\text{lin}}(k, z), \quad (8)$$

with $\tilde{v}(k|m)$ being the Fourier transform of $\rho(\mathbf{x}|m)/\bar{\rho}$ and $\langle g_S \rangle = \int d\mathcal{L} \Phi \mathcal{L}$. In Eqs. (8) a relation between the source luminosity \mathcal{L} and the host-halo mass m is required. We compute the source bias b_S through the halo bias by means of $b_S(\mathcal{L}, z) = b_h(M_h(\mathcal{L}), z)$, for which we need again a relation between host-halo mass and source luminosity. On the other hand, since at low redshift and in the mass-range of interest $b_h \sim 1$, the 2-halo term is only very mildly dependent on the description of $M_h(\mathcal{L})$. For a power-law spectrum with index α , the window function is:

$$W^{\gamma s}(E_\gamma, z) = \frac{A_S(z) \langle g_S(z) \rangle}{4\pi E_0^2} \int_{E_\gamma}^\infty dE \left(\frac{E}{E_0} \right)^{-\alpha} e^{-\tau(E, z)},$$

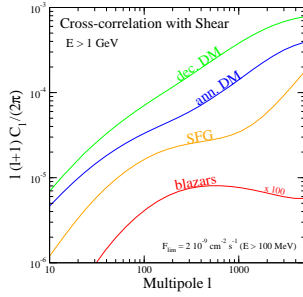


FIG. 3. Cross-correlation of the cosmic shear with the γ -ray emission for the four benchmark models described in the text (with a γ -ray threshold expected for Fermi-LAT after 5 years of exposure and a distribution of background sources for lensing as in Euclid). Each contribution is normalized by multiplying Eq. (2) by $\langle I_j \rangle / \langle I_{\text{EGB}} \rangle$ to make them additive.

where $E_0 = 100$ MeV and A_S is a factor that depends on which specific luminosity is chosen as the characterizing parameter (as we will describe below).

The GLF of blazars is computed following the model described in [39] with the AGN X-ray luminosity function from [40] and with the numerical value of parameters derived in [28] by fitting Fermi-LAT data on EGB diffuse emission and anisotropies. The spectrum is taken to be a power-law with $\alpha = 2.2$, and \mathcal{L} is the γ -ray luminosity at 100 MeV (which leads to $A_S = (1+z)^{-\alpha}$). We assume that no blazars fainter than the luminosity cutoff $\mathcal{L}_{\text{min}} = 10^{42}$ erg/s can exist at any redshift, while $\mathcal{L}_{\text{max}}(z)$ is the maximum luminosity above which a blazar can be resolved (for 5-yr Fermi-LAT it is computed taking $F_{\text{max}} = 2 \cdot 10^{-9} \text{ cm}^{-2} \text{ s}^{-1}$ for $E > 100$ MeV which is the value assumed in Figs. (2–4)). The relation between halo-mass and blazar luminosity can be described through $M_h = 10^{11.3} M_\odot (\mathcal{L}/10^{44.7} \text{ erg/s})^{1.7}$ following [41] where the blazar γ -ray luminosity is linked to the mass of the associated supermassive black hole, which is in turn related to the halo mass. The description of $M_h(\mathcal{L})$ suffers from sizable uncertainties (see Appendix) which propagate to the prediction of the 1-halo term. However, as we will see later, the blazar contribution is largely subdominant, thus such uncertainties do not affect our conclusions.

For the GLF of SFGs, we follow results from the Fermi-LAT Collaboration [42], which are based on the infrared (IR) luminosity function derived in [43], and the rescaling relation between γ -ray and IR luminosity obtained analyzing resolved SFGs [42]. The spectrum is assumed to be a power-law with $\alpha = 2.7$, similarly to the Milky Way case, and \mathcal{L} is the γ -ray luminosity between 0.1 and 100 GeV (which leads to $A_S = (\alpha - 2)/(1 + z)^2$). The relation $M_h(\mathcal{L})$ could, in principle, be computed from the relation between γ -ray luminosity and star formation rate (SFR) [42], the Schmidt-Kennicutt law (connecting SFR and gas density), and the ratio of gas to total galactic mass. This leads to different relations

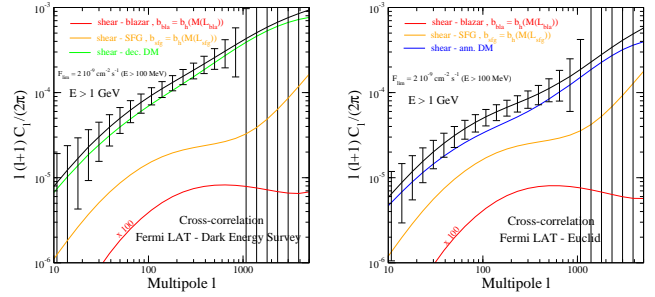


FIG. 4. *Left*: Cross-correlation between cosmic shear and γ -ray emission, for different classes of γ -ray emitters. DES is taken as the reference galaxy survey. Error bars are estimated for the total signal (in black). *Right*: Same as in the left panel but for annihilating DM, with Euclid as the reference galaxy survey.

for each different subpopulation of SFGs (e.g., ellipticals are much brighter than spirals of the same mass); on the other hand we do not have γ -ray data to compute the specific GLF of the sub-populations, thus we have to derive an effective averaged relation. Assuming a power-law scaling $M_h = \mathcal{A} \cdot 10^{12} M_\odot (\mathcal{L}/10^{39} \text{ erg/s})^\mathcal{B}$ and a maximum galactic mass of $M_{\text{max}} = 10^{14} M_\odot$, we can find \mathcal{A} and \mathcal{B} using, e.g., the Milky Way data ($M_h \simeq 10^{12} M_\odot$ and $\mathcal{L} \simeq 10^{39} \text{ erg/s}$) and requiring that the mass associated to the maximum luminosity $\sim 10^{43} \text{ erg/s}$ (this can be computed from the maximum measured IR luminosity rescaled to γ -ray frequency) not to exceed M_{max} . We found $\mathcal{A} \simeq 1$ and $\mathcal{B} \simeq 0.5$. This is just a simple model, and we estimated the impact of the associated uncertainty on the 1-halo term (by varying \mathcal{A} and \mathcal{B} within reasonable ranges) to be $\mathcal{O}(1)$ (see Appendix).

Results. For the sake of clearness we focus on a benchmark annihilating (decaying) DM scenario, where the WIMP has a mass of 100 GeV (200 GeV), annihilation (decay) rate of $(\sigma_a v) = 8 \cdot 10^{-26} \text{ cm}^3/\text{s}$ ($\tau_d = 3 \cdot 10^{26} \text{ s}$) and dominant final state $\bar{b}b$. The characteristics of the DM particle are chosen to saturate (at least in one particular energy range) the EGB emission, without violating the experimental constraints. In particular, we note that, although we take DM to be a significant component of the EGB at $E \gtrsim 1$ GeV in Fig. 1a, it is basically impossible to obtain an evidence for DM from the angular PS of γ -rays alone because the latter is dominated by the blazar contribution.

In Fig. 2 we show the ingredients of Eq. (2) for the computation of the shear/ γ -ray cross-correlation angular PS: the window function for the cosmic shear signal nicely overlaps with the DM window function, both for annihilating and decaying DM, while this happens only at intermediate redshifts for the SFG window function and only at high redshifts for the case of blazars. This suggests that a tomographic approach could be a powerful strategy to further disentangle different contributions in the angular PS (this will be pursued in

a future work [44]). The shear signal is stronger for large masses. The same is true also for the γ -ray signal from DM and this fact gives a large 1-halo contribution which dominates starting from $k \lesssim 1 h/\text{Mpc}$ in Fig. 2b. Galaxies have masses $\lesssim 10^{14} M_\odot$, thus they correlate with the shear signal of lower-mass halos and the 1-halo contribution becomes important at slightly smaller scale $k \gtrsim 1 h/\text{Mpc}$. Since the bulk of unresolved blazars in 5-yr Fermi-LAT will be hosted in relatively small halos at large redshift, the 1-halo term of the blazar/shear PS is suppressed. Thus, an important result is that, since both the shear and DM-induced γ -ray signals are stronger for large halos, their cross-correlation is more effective with respect to the case of astrophysical sources. This, together with the sizable overlapping of the DM γ -ray and shear window functions at low redshift, leads to the expectation of a sizable DM signal in the angular PS, which is indeed what we find in Fig. 3. For $\ell \lesssim 100$ the 2-halo term dominates for all the sources, thus the relative size is roughly given by the relative contribution in the total EGB emission. At $\ell \gtrsim 100$, the 1-halo term starts to be important in the DM case which grows more rapidly than the astrophysical sources. At $\ell \gtrsim 10^3$, the 1-halo term takes over also in the SFG spectrum which is brought again close to the DM curve. Blazars are largely subdominant in the whole range of multipoles.

The observational forecasts for the cross-correlation between DES or Euclid and Fermi-LAT are shown in Fig. 4 for the benchmark models considered in this work (for error estimates see e.g. [31], and observational performances are taken from [9, 10, 45]). The figure shows that, provided the DM is a significant component of the total γ -ray EGB as in our assumptions, a DM signal can be disentangled in the angular PS at $\ell \lesssim 10^3$.

Conclusions. In this Letter, we discussed the cross-correlation angular power spectrum of weak lensing cosmic shear and γ -rays produced by WIMP annihilations/decays and astrophysical sources. We showed that this method can provide novel information on the composition of the EGB. Since the shear signal is stronger for structures of larger masses and most of the γ -ray emission from decaying and (in many models of) annihilating DM is also produced in large mass halos, their cross-correlation is typically stronger than the case of astrophysical sources (which are associated to galactic-mass halos). Forthcoming surveys like DES and Euclid can thus potentially provide evidence for WIMPs.

Acknowledgements. We thank Anne Green for useful comments. NF and MR acknowledge the italian PRIN 2008 grant number 2008NR3EBK, together with the INFN grant FA51. NF acknowledges support of Spanish grant MULTIDARK CSD2009-00064. MF is supported by a Leverhulme Trust grant. SC acknowledges support

from FCT-Portugal under grant PTDC/FIS/100170/2008. SC work is funded by FCT-Portugal under Post-Doctoral Grant SFRH/ BPD/ 80274/ 2011.

-
- [1] N. Kaiser, *Astrophys. J.* **388** (1992) 272.
 - [2] M. Bartelmann *et al.*, *Phys. Rept.* **340** (2001) 291.
 - [3] D. Munshi *et al.* *Phys. Rept.* **462** (2008) 67.
 - [4] M. Bartelmann, *Class. Quant. Grav.* **27** (2010) 233001.
 - [5] E. Julio *et al.*, *Astrophys. J.* **750** (2012) 37.
 - [6] I. Tereno *et al.*, *Astron. Astrophys.* **530** (2011) A68.
 - [7] S. de la Torre *et al.*, arXiv:1007.1984 [astro-ph.CO].
 - [8] T. Schrabback *et al.*, *Astron. Astrophys.* **516** (2010) A63.
 - [9] T. Abbott *et al.* [DES Collab.], astro-ph/0510346.
 - [10] R. Laureijs *et al.*, arXiv:1110.3193; L. Amendola *et al.* [Euclid Theory Working Group Collab.], arXiv:1206.1225; <http://www.euclid-ec.org>.
 - [11] A. Abdo *et al.* [Fermi-LAT Collab.], *Phys. Rev. Lett.* **104** (2010) 101101.
 - [12] K. Abazajian *et al.* *Phys. Rev. D* **84** (2011) 103007.
 - [13] F. Stecker and T. Venters, *Astrophys. J.* **736** (2011) 40.
 - [14] J. Singal, V. Petrosian, M. Ajello, *Ap. J.* **753** (2012) 45.
 - [15] M. Ackermann *et al.* [Fermi LAT Collab.], *Astrophys. J.* **755** (2012) 164.
 - [16] B. Lacki *et al.*, arXiv:1206.0772.
 - [17] Y. Inoue, *Astrophys. J.* **733** (2011) 66.
 - [18] F. Massaro and M. Ajello, arXiv:1102.0774.
 - [19] P. Ullio *et al.* *Phys. Rev. D* **66** (2002) 123502.
 - [20] J. Zavala *et al.*, *MNRAS* **405** (2010) 593.
 - [21] M. Cirelli *et al.* *JCAP* **1103** (2011) 051 [Erratum-ibid. **1210** (2012) E01].
 - [22] J. Zavala *et al.* *Phys. Rev. D* **83** (2011) 123513.
 - [23] M. Fornasa *et al.*, arXiv:1207.0502.
 - [24] A. Abdo *et al.* [Fermi-LAT Collab.], *JCAP* **1004** (2010) 014.
 - [25] F. Calore *et al.*, *Phys. Rev. D* **85** (2012) 023004.
 - [26] M. Ackermann *et al.* [Fermi LAT Collab.], *Phys. Rev. D* **85** (2012) 083007.
 - [27] A. Cuoco *et al.*, *Phys. Rev. D* **86** (2012) 063004.
 - [28] J. Harding and K. Abazajian, *JCAP* **1211** (2012) 026.
 - [29] R. Scherrer and E. Bertschinger, *Ap. J.* **381**, 349 (1991).
 - [30] S.'i. Ando, E. Komatsu, *Phys. Rev. D* **73** (2006) 023521.
 - [31] S.'i. Ando *et al.*, *Phys. Rev. D* **75** (2007) 063519.
 - [32] L. Fu *et al.*, *Astron. Astrophys.* **479** (2008) 9.
 - [33] A. Cooray and R. K. Sheth, *Phys. Rept.* **372** (2002) 1.
 - [34] R. Sheth and G. Tormen, *MNRAS* **308** (1999) 119.
 - [35] J. C. Munoz-Cuartas *et al.* arXiv:1007.0438.
 - [36] J. Navarro *et al.*, *Astrophys. J.* **490** (1997) 493.
 - [37] F. Stecker *et al.*, *Astrophys. J.* **658** (2007) 1392.
 - [38] M. Kamionkowski *et al.*, *Phys. Rev. D* **81** (2010) 043532.
 - [39] Y. Inoue and T. Totani, *Astrophys. J.* **702** (2009) 523 [Erratum-ibid. **728** (2011) 73].
 - [40] Y. Ueda *et al.* *Astrophys. J.* **598** (2003) 886.
 - [41] S.'i. Ando *et al.* *MNRAS* **376** (2007) 1635.
 - [42] M. Ackermann *et al.* [Fermi LAT Collab.], *Astrophys. J.* **755** (2012) 164.
 - [43] G. Rodighiero *et al.*, arXiv:0910.5649.
 - [44] S. Camera, M. Fornasa, N. Fornengo and M. Regis, in preparation.
 - [45] W. Atwood *et al.* [LAT Collab.], *Ap. J.* **697** (2009) 1071.
 - [46] R. Takahashi *et al.* *Astrophys. J.* **761** (2012) 152.

General Formalism

Expanding the intensity fluctuations of Eq. (1) in spherical harmonics, $\delta I_g(\vec{n}) \equiv I_g(\vec{n}) - \langle I_g \rangle = \langle I_g \rangle \sum_{\ell m} a_{\ell m} Y_{\ell m}(\vec{n})$, and using orthonormal relation for $Y_{\ell m}$, one obtains the expression for the (dimensionless) $a_{\ell m}$ coefficients:

$$a_{\ell m} = \frac{1}{\langle I_g \rangle} \int d\vec{n} \delta I_g(\vec{n}) Y_{\ell m}^*(\vec{n}) = \frac{1}{\langle I_g \rangle} \int d\vec{n} d\chi f_g(\chi, \mathbf{r}) W(\chi) Y_{\ell m}^*(\vec{n}), \quad (9)$$

where $f_g \equiv g/\langle g \rangle - 1$. Then, through the spatial Fourier transformation of f_g and making use of the Rayleigh formula, we get:

$$\begin{aligned} a_{\ell m} &= \frac{1}{\langle I_g \rangle} \int d\vec{n} d\chi \frac{d\mathbf{k}}{(2\pi)^3} \hat{f}_g(\chi, \mathbf{k}) e^{i\mathbf{k} \cdot \mathbf{r}} W(\chi) Y_{\ell m}^*(\vec{n}) \\ &= \frac{1}{\langle I_g \rangle} \int d\vec{n} d\chi \frac{d\mathbf{k}}{2\pi^2} \hat{f}_g(\chi, \mathbf{k}) \left[\sum_{\ell' m'} i^{\ell'} j_{\ell'}(k\chi) Y_{\ell' m'}^*(\hat{\mathbf{k}}) Y_{\ell' m'}(\vec{n}) \right] W(\chi) Y_{\ell m}^*(\vec{n}) \\ &= \frac{i^\ell}{\langle I_g \rangle} \int d\chi W(\chi) \int \frac{d\mathbf{k}}{2\pi^2} \hat{f}_g(\chi, \mathbf{k}) j_\ell(k\chi) Y_{\ell m}^*(\hat{\mathbf{k}}). \end{aligned} \quad (10)$$

The angular PS is then $C_\ell^{(ij)} = \langle \sum_m a_{\ell m}^{(i)} a_{\ell m}^{(j)*} \rangle$, where $i, j = 1, 2$ label the signals (e.g., γ -rays and cosmic-shear), and $C_\ell^{(12)} = C_\ell^{(21)}$ (which can be easily understood from $a_\ell = (-1)^m a_{\ell - m}^*$)¹. Using Eq. (10), it takes the form:

$$\begin{aligned} C_\ell^{(ij)} &= \frac{1}{\langle I_i \rangle \langle I_j \rangle} \int d\chi W_i(\chi) \int d\chi' W_j(\chi') \int \frac{d\mathbf{k}}{2\pi^2} \int \frac{d\mathbf{k}'}{2\pi^2} \langle \hat{f}_{g_i}(\chi, \mathbf{k}) \hat{f}_{g_j}^*(\chi', \mathbf{k}') \rangle j_\ell(kr) j_{\ell'}(k'r') Y_{\ell m}(\hat{\mathbf{k}}) Y_{\ell' m'}^*(\hat{\mathbf{k}}') \\ &= \frac{2}{\pi \langle I_i \rangle \langle I_j \rangle} \int d\chi W_i(\chi) \int d\chi' W_j(\chi') \int d\mathbf{k} P_{ij}(k, \chi, \chi') j_\ell(kr) j_{\ell'}(kr') Y_{\ell m}(\hat{\mathbf{k}}) Y_{\ell' m'}^*(\hat{\mathbf{k}}) \\ &= \frac{2}{\pi \langle I_i \rangle \langle I_j \rangle} \int d\chi W_i(\chi) \int d\chi' dk k^2 W_j(\chi') P_{ij}(k, \chi, \chi') j_\ell(kr) j_{\ell'}(kr') \\ &= \frac{1}{\langle I_i \rangle \langle I_j \rangle} \int \frac{d\chi}{\chi^2} W_i(\chi) W_j(\chi) P_{ij}(k = \ell/\chi, \chi). \end{aligned}$$

where in the second step we introduced the definition of P_{ij} through $\langle \hat{f}_{g_i}(\chi, \mathbf{k}) \hat{f}_{g_j}^*(\chi', \mathbf{k}') \rangle = (2\pi)^3 \delta^3(\mathbf{k} - \mathbf{k}') P_{ij}(k, \chi, \chi')$, and in the last step we assumed the Limber approximation to hold for such PS.

So far, we just re-derived the general expression for the cross-correlation angular PS in Eq. (2). The next step is to compute the form for the specific PS P_{ij} of interest. The PS is the Fourier transform of the 2PCF in real space, $\xi^{(2)}(\mathbf{x} - \mathbf{y}) \equiv \langle f_{g_i}(\mathbf{x}) f_{g_j}(\mathbf{y}) \rangle$. To compute it we follow [29] and assume the density field can be written as the sum of independent seeds:

$$f(\mathbf{x}) = \sum_i f(m_i, \mathbf{x} - \mathbf{x}_i) = \int dm \int d^3 \mathbf{x}' \sum_i \delta^3(\mathbf{x}' - \mathbf{x}_i) \delta(m - m_i) f(m, \mathbf{x} - \mathbf{x}'), \quad (11)$$

where i labels the seeds, δ is the Dirac-delta function, and we take the mass m to be the parameter which characterizes the seeds. The seed density is given by $dn/dm = \langle \sum_i \delta^3(\mathbf{x} - \mathbf{x}_i) \delta(m - m_i) \rangle$, where, here, $\langle \rangle$ denotes the ensemble average over of all possible seed distributions.

Using Eq. (11), the 2PCF $\langle f_1(\mathbf{x}) f_2(\mathbf{y}) \rangle$ is given by:

$$\xi^{(2)}(\mathbf{x}, \mathbf{y}) = \int dm_1 dm_2 d^3 \mathbf{x}_1 d^3 \mathbf{x}_2 \langle \sum_i \delta^3(\mathbf{x}_1 - \mathbf{x}_i) \delta(m_1 - m_i) \sum_j \delta^3(\mathbf{x}_2 - \mathbf{x}_j) \delta(m_2 - m_j) \rangle f_1(m_1, \mathbf{x} - \mathbf{x}_1) f_2(m_2, \mathbf{y} - \mathbf{x}_2). \quad (12)$$

¹ Note that if there are k components contributing to a signal y (e.g., blazars and DM for γ -rays), one has $I_y = \sum_k I_k$ and $\delta I_y / I_y = \sum_k \delta I_k / I_y$, which leads to $a_{\ell m}^{(y)} = \sum_k f_k a_{\ell m}^k$, where

$f_k = I_k / I_y$ is the fraction of contribution from each component.

The correlation of a seed with mass m_1 at position \mathbf{x}_1 with a different seed with mass m_2 at position \mathbf{x}_2 is provided by the seed 2PCF $\xi_s^{(2)}(m_1, m_2, \mathbf{x}_1, \mathbf{x}_2)$, and it is not difficult to see that:

$$\langle \sum_i \delta^3(\mathbf{x}_1 - \mathbf{x}_i) \delta(m_1 - m_i) \sum_j \delta^3(\mathbf{x}_2 - \mathbf{x}_j) \delta(m_2 - m_j) \rangle = \frac{dn}{dm_1} \frac{dn}{dm_2} [1 + \xi_s^{(2)}(m_1, m_2, \mathbf{x}_1, \mathbf{x}_2)] + \frac{dn}{dm_1} \delta^3(\mathbf{x}_1 - \mathbf{x}_2) \delta(m_1 - m_2) \quad (13)$$

which leads to:

$$\begin{aligned} \xi^{(2)}(\mathbf{x}, \mathbf{y}) &= \int dm d^3\mathbf{x}_1 \frac{dn}{dm} f_1(\mathbf{x} - \mathbf{x}_1, m) f_2(\mathbf{y} - \mathbf{x}_1, m) \\ &+ \int dm_1 dm_2 d^3\mathbf{x}_1 d^3\mathbf{x}_2 \frac{dn}{dm_1} \frac{dn}{dm_2} f_1(\mathbf{x} - \mathbf{x}_1, m_1) f_2(\mathbf{y} - \mathbf{x}_2, m_2) \xi_s^{(2)}(m_1, m_2, \mathbf{x}_1, \mathbf{x}_2) . \end{aligned} \quad (14)$$

Remembering that $P(k)$ is the Fourier transform of $\xi^{(2)}(\mathbf{x}, \mathbf{y})$ and writing f_i in terms of their Fourier transforms \hat{f}_i , one obtains:

$$P_{ij}(k) = \int dm \frac{dn}{dm} \hat{f}_i^*(k|m) \hat{f}_j(k|m) + \int dm_1 dm_2 \frac{dn}{dm_1} \frac{dn}{dm_2} \hat{f}_i^*(k|m_1) \hat{f}_j(k|m_2) P^{(s)}(k, m_1, m_2) , \quad (15)$$

where the PS of the seed distribution $P^{(s)}$ is the Fourier transform of $\xi_s^{(2)}$.

Our reference case obviously concerns mass density fluctuations. Therefore $\xi_s^{(2)}$ is the (homogeneous and isotropic) linear correlation function of matter (note that it has to be the linear one since in Eq. (11) we wrote the density field as a linear superposition of seeds).

For the objects considered in the following (DM halos and astrophysical sources), we will assume (as usually done) that their 2PCF ξ_{ij} can be related to the linear correlation function of matter by means of $\xi_{ij}^{(2)}(\mathbf{x}_i, \mathbf{x}_j|m_1, m_2) \approx b_i(m_1) b_j(m_2) \xi_{\text{lin}}^{(2)}(|\mathbf{x}_i - \mathbf{x}_j|)$ where $b_i(m)$ is the linear bias between the object i and matter. Thus using $P^{(s)}(k, m_1, m_2) = b_i(m_1) b_j(m_2) P^{\text{lin}}(k)$, we finally arrive to Eqs. (3) and (4).

Three-dimensional power spectra

In this section, we explicitly write down and plot the auto- and cross-correlation three-dimensional power spectra, which can be derived from Eqs. (3) and (4) by using the functions g_i introduced in the main text.

Auto-correlation

For the cases of weak lensing shear and γ -rays from decaying DM, the density field of the source is given by the density contrast $\delta(\mathbf{x})$, i.e., $f_d(\mathbf{x}) = \delta(\mathbf{x})$ and $f_\kappa(\mathbf{x}) = \delta(\mathbf{x})$. Therefore the sum of the one and two-halo terms in Eqs. (3) and (4) provides the non-linear matter PS $P^{\delta\delta}$:

$$P_{\delta\delta}^{1h}(k) = \int dm \frac{dn}{dm} \tilde{v}(k|m)^2 , \quad P_{\delta\delta}^{2h}(k) = \left[\int dm \frac{dn}{dm} b_h(m) \tilde{v}(k|m) \right]^2 P^{\text{lin}}(k) , \quad (16)$$

with $\tilde{v}(k|m)$ being the Fourier transform of $\rho(\mathbf{x}|m)/\bar{\rho}$. In order to validate our method, we can thus compare our halo-model-based predictions for the matter PS with latest results from high-resolution N -body simulations [46]. This is shown in Fig. 5a. A very good agreement (in particular at low redshift which is the most relevant epoch for our purposes) is achieved.

Approximating astrophysical sources as point sources, we have $g_S(\mathcal{L}, \mathbf{x} - \mathbf{x}') = \mathcal{L} \delta^3(\mathbf{x} - \mathbf{x}')$, and Eqs. (3) and (4) become:

$$P_{\gamma_S \gamma_S}^{1h}(k, z) = \int_{\mathcal{L}_{\min}(z)}^{\mathcal{L}_{\max}(z)} d\mathcal{L} \Phi(\mathcal{L}, z) \left(\frac{\mathcal{L}}{\langle g_S \rangle} \right)^2 , \quad P_{\gamma_S \gamma_S}^{2h}(k, z) = \left[\int_{\mathcal{L}_{\min}(z)}^{\mathcal{L}_{\max}(z)} d\mathcal{L} \Phi(\mathcal{L}, z) b_S(\mathcal{L}, z) \frac{\mathcal{L}}{\langle g_S \rangle} \right]^2 P^{\text{lin}}(k, z) . \quad (17)$$

Since the term in the square-brackets does not depend on k (because of the point-source approximation) and Eq. (5) becomes $\langle g_S \rangle = \int d\mathcal{L} \Phi \mathcal{L}$, the 2-halo term is just a rescaled version of P^{lin} with the rescaling factor due to the bias

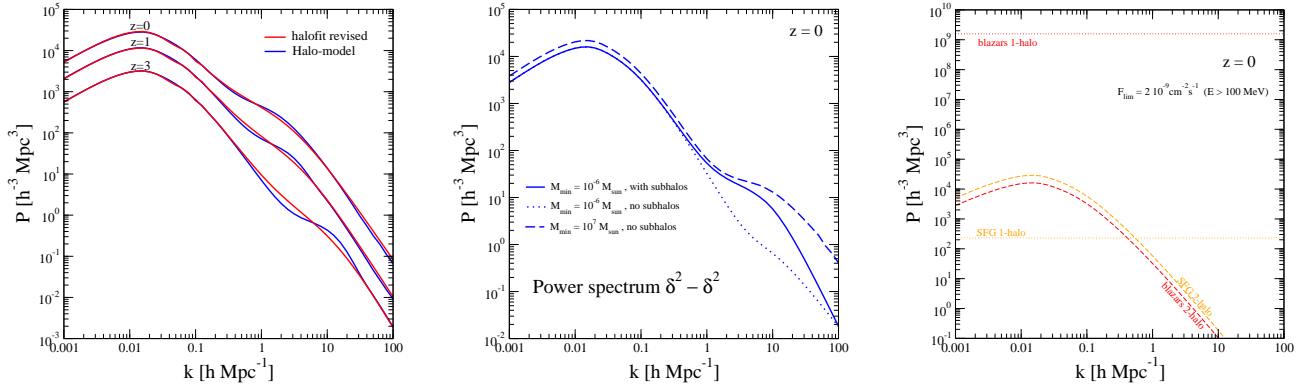


FIG. 5. *Left*: Comparison between the non-linear 3-dimensional matter PS obtained with the halo-model considered in this paper and the revised halo-fit results from high-resolution N -body simulations of [46] at different redshift. *Central*: Auto-correlation 3-dimensional γ -ray PS of blazars and SFGs at $z = 0$. For blazars the 1-halo term strongly dominates. *Right*: Auto-correlation 3-dimensional PS of annihilating DM in the three scenarios described in the text at $z = 0$.

(so possibly varying with z). The 1-halo term is constant in k , namely it is a “Poisson-noise” term. The results for the blazar and SFG benchmark models described in the main text are shown in Fig. 5c.

The signal of annihilating DM scales with ρ^2 , so to derive the associated angular PS, we can again use the formalism outlined in the previous section by just squaring the r.h.s. in Eq. (11) (with f in the r.h.s. still given by ρ). The correlation function would then lead to a term proportional to:

$$\langle \sum_i \delta^3(\mathbf{x}_1 - \mathbf{x}_i) \delta(m_1 - m_i) \sum_j \delta^3(\mathbf{x}_2 - \mathbf{x}_j) \delta(m_2 - m_j) \sum_k \delta^3(\mathbf{x}_3 - \mathbf{x}_k) \delta(m_3 - m_k) \sum_l \delta^3(\mathbf{x}_4 - \mathbf{x}_l) \delta(m_4 - m_l) \rangle, \quad (18)$$

which can be in turn expanded into four-, three-, and two-point seed correlation functions. However, since halos (described by $\rho(\mathbf{x}|m)$) are mutually exclusive, an annihilation can only occur if the two particles are within the same halo. This implies that all the terms other than the 1- and 2-halo contributions (which are the same appearing in the r.h.s. of Eq. 13) vanish. Eq. (14) does not change, with f_a now being $\rho(\mathbf{x}|m)^2 / \langle \rho^2 \rangle$. The auto-correlation PS is thus given by:

$$P_{\gamma_a \gamma_a}^{1h}(k) = \int_{m_{\min}}^{m_{\max}} dm \frac{dn}{dm} \left(\frac{\tilde{u}(k|m)}{\Delta^2} \right)^2; \quad P_{\gamma_a \gamma_a}^{2h}(k) = \left[\int_{m_{\min}}^{m_{\max}} dm \frac{dn}{dm} b_h(m) \frac{\tilde{u}(k|m)}{\Delta^2} \right]^2 P^{\text{lin}}(k) \quad (19)$$

with $\tilde{u}(k|m)$ being the Fourier transform of $\rho^2(\mathbf{x}|m)/\bar{\rho}^2$. Our results are only very mildly dependent on the upper mass cutoff (which we set to be $m_{\max} = 10^{18} M_\odot$), while crucial ingredients are the minimum halo mass m_{\min} and the DM clustering at very small masses. In Fig. 5c, we show three examples: two models having $m_{\min} = 10^{-6} M_\odot$ (which is the typical WIMP free-streaming mass) with/without substructures (the latter described as mentioned in the main text) and $m_{\min} = 10^7 M_\odot$ (which is the minimum halo mass currently inferred from dynamical measurements) without substructures.

Cross-correlation

For the cross-correlation between shear and decaying DM, the 3-dimensional PS $P_{\kappa \gamma_d}$ is simply the non-linear matter PS $P^{\delta\delta}$.

The case of cross-correlation of γ -rays from astrophysical sources with decaying DM is analogous to the case of γ -rays from astrophysical sources with weak lensing shear signal, both given by:

$$P_{\gamma_S \delta}^{1h}(k, z) = \int_{\mathcal{L}_{\min}(z)}^{\mathcal{L}_{\max}(z)} d\mathcal{L} \Phi(\mathcal{L}, z) \frac{\mathcal{L}}{\langle g_S \rangle} \tilde{v}(k|m(\mathcal{L})) \quad (20)$$

$$P_{\gamma_S \delta}^{2h}(k, z) = \left[\int_{\mathcal{L}_{\min}(z)}^{\mathcal{L}_{\max}(z)} d\mathcal{L} \Phi(\mathcal{L}, z) b_S(\mathcal{L}, z) \frac{\mathcal{L}}{\langle g_S \rangle} \right] \left[\int_{m_{\min}}^{m_{\max}} dm \frac{dn}{dm} b_h(m) \tilde{v}(k|m) \right] P^{\text{lin}}(k, z). \quad (21)$$

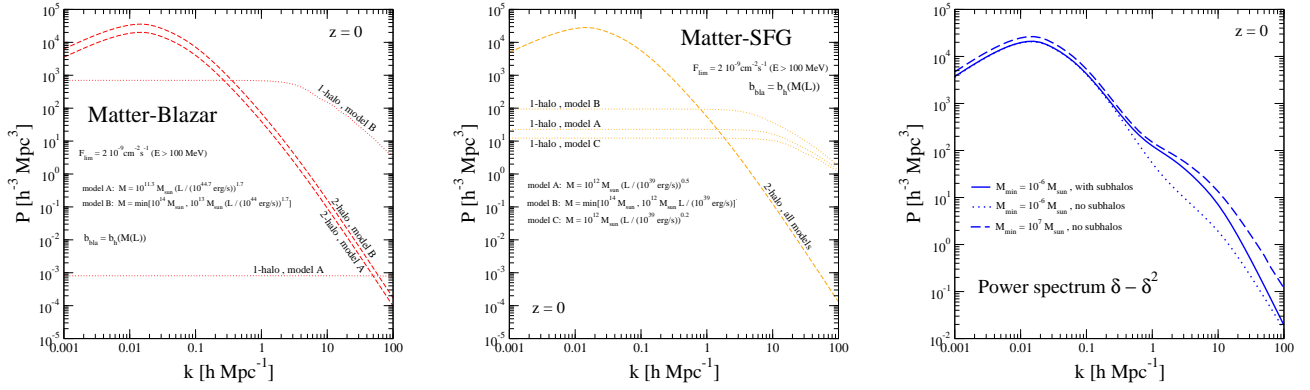


FIG. 6. *Left*: 3-dimensional cross-correlation PS between shear and γ -rays from blazars at $z = 0$. The two models for $m(\mathcal{L})$ are taken from Ref. [41] (here \mathcal{L} is the γ -ray luminosity at 100 MeV). *Central*: Same of left panel but for SFGs (with \mathcal{L} now being the γ -ray luminosity between 100 MeV and 100 GeV). *Right*: 3-dimensional cross-correlation PS between shear and annihilating DM in the three scenarios described in the text at $z = 0$.

Results are plotted in Fig. 6 for the benchmark models described in the main text and highlighting the impact of $m(\mathcal{L})$ by showing different choices for such relation. We assume the maximum mass for a galaxy to be $M_{\max} = 10^{14} M_{\odot}$. In the case of blazars, the 1-halo term strongly depends on $m(\mathcal{L})$. On the other hand, even with a dramatic increase of its level (model B) with respect to our benchmark case (model A), the contribution of blazars in the cross-correlation angular PS of Fig. 3 remains subdominant. The dependence of the SFG-shear PS on the $m(\mathcal{L})$ relation is milder.

The cross-correlation power spectra involving the annihilating DM case can be computed from the term

$$\left\langle \sum_i \delta^3(\mathbf{x}_1 - \mathbf{x}_i) \delta(m_1 - m_i) \sum_j \delta^3(\mathbf{x}_2 - \mathbf{x}_j) \delta(m_2 - m_j) \sum_k \delta^3(\mathbf{x}_3 - \mathbf{x}_k) \delta(m_3 - m_k) \right\rangle, \quad (22)$$

and again noting that only terms in the r.h.s. of Eq. (13) survive, leading again to Eq. (14) (see also Appendix B in [31]). This leads to:

$$\begin{aligned} P_{\delta\gamma_a}^{1h}(k) &= \int_{m_{\min}}^{m_{\max}} dm \frac{dn}{dm} \tilde{v}(k|m) \frac{\tilde{u}(k|m)}{\Delta^2} \\ P_{\delta\gamma_a}^{2h}(k) &= \left[\int_{m_{\min}}^{m_{\max}} dm \frac{dn}{dm} b_h(m) \tilde{v}(k|m) \right] \left[\int_{m_{\min}}^{m_{\max}} dm \frac{dn}{dm} b_h(m) \frac{\tilde{u}(k|m)}{\Delta^2} \right] P^{\text{lin}}(k), \end{aligned} \quad (23)$$

and the 3-dimensional PS of cross-correlation of annihilating DM with shear and decaying DM are again analogous. Results are shown in Fig. 6 for the same three annihilating DM models of Fig. 5.

For completeness, although not directly related to the computations shown in this work, we provide the PS in the case of cross-correlation of γ -rays between astrophysical sources and annihilating DM:

$$\begin{aligned} P_{\gamma_S\gamma_a}^{1h}(k, z) &= \int_{\mathcal{L}_{\min}(z)}^{\mathcal{L}_{\max}(z)} d\mathcal{L} \Phi(\mathcal{L}, z) \frac{\mathcal{L}}{\langle g_S \rangle} \frac{\tilde{u}(k|m(\mathcal{L}))}{\Delta^2} \\ P_{\gamma_S\gamma_a}^{2h}(k, z) &= \left[\int_{\mathcal{L}_{\min}(z)}^{\mathcal{L}_{\max}(z)} d\mathcal{L} \Phi(\mathcal{L}, z) b_S(\mathcal{L}, z) \frac{\mathcal{L}}{\langle g_S \rangle} \right] \left[\int_{m_{\min}}^{m_{\max}} dm \frac{dn}{dm} b_h(m) \frac{\tilde{u}(k|m)}{\Delta^2} \right] P^{\text{lin}}(k, z). \end{aligned} \quad (24)$$